THE CHALLENGE OF THE PERFORMANCE-BASED APPROACH FOR THE DESIGN OF REINFORCED CONCRETE STRUCTURES IN CHLORIDE BEARING ENVIRONMENT

Federica Lollini[1*], Maddalena Carsana[2], Matteo Gastaldi[3], Elena Redaelli[4], Luca Bertolini[5]

Politecnico di Milano, Department of Chemistry, Materials and Chemical Engineering "Giulio Natta", via Mancinelli, 7 - 20131 Milano, Italy

E-mail: [1]federica.lollini@polimi.it, [2]maddalena.carsana@polimi.it, [3]matteo.gastaldi@polimi.it, [4]elena.redaelli@polimi.it, [5]luca.bertolini@polimi.it

[*] Corresponding author

tel: +39 02 2399 3144

fax: +39 02 2399 3180

Abstract: The performance-based approach, published by the International Federation for Structural Concrete (*fib*), was applied for the design of a RC element in a marine environment, with corrosion resistant reinforcement, to analyse the potentiality of the model as well as the possible reasons which limit its use. Results showed that the *fib* model allows to compare different solutions and to consider the benefits connected with the use of preventative measures. However the definition of reliable values for some input parameters, as the critical chloride threshold for corrosion resistant reinforcement, is demanded to the designer and this aspect clearly limits a widespread use.

Highlights:

The probabilistic model proposed by *fib* was used for the design of RC element in the splash zone.

Different combinations of concrete composition and type of reinforcement were considered.

Definition of input parameters for the model was a critical issue.

Values for the input parameters were determined through literature survey.

The model sensitivity to the estimated input values depended on the type of steel.

keywords: probabilistic approach, service life, durability, chlorides, stainless steel, galvanized steel

1. Introduction

In reinforced concrete (RC) structures, corrosion of embedded steel is the main form of premature damage worldwide. Corrosion may take place due to carbonation of concrete or chloride penetration from seawater or de-icing salts and may have several consequences on the serviceability and safety of reinforced concrete structures leading, for instance, to cracking or spalling in localized areas [1-6]. When one of these adverse events occurs, a repair becomes necessary to restore safety or serviceability targets. As a result, owners of civil infrastructures as well as buildings have to spend an increasing percentage of their budgets on repair and maintenance of existing RC structures. Thus, there is an increasing interest in extending the service life of new RC structures and reduce maintenance and repair costs over the design service life.

Numerous strategies are now available for enhancing the service life of reinforced structures, as, for instance, low-permeability concrete, coatings, cathodic prevention or corrosion resistant steel (e.g.

stainless steel and galvanized steel) [1]. Higher initial construction costs associated to the use of these preventative measures, under specific environmental conditions, may lead to remarkable reductions in the future repair costs. The selection of the most suitable design solution amongst the wide range of preventative approaches nowadays available requires a quantification of all the associated costs in comparison to the expected extension of the life of the structure. Hence, the first essential step in the cost-benefit evaluation of any preventative measure is the prediction of its actual contribution in increasing the service life. This can only be achieved by predicting the performance of the structure as a function of time and the environmental actions, i.e. through service life modelling. At this aim, several models have been proposed in the literature [1]. Nowadays, performance-based approaches are becoming more popular, since they aim at a tailor-made design in which every structural element should be specifically designed in a way that it can withstand the actual local conditions of exposure during the required service life. Among the models proposed in the recent years, the "Model Code for Service Life Design", issued by the International Federation for Structural Concrete (*fib*) in 2006 [7], is often used being considered one of the most authoritative [8]. This includes a probabilistic performance-based approach for the modelling of the effects of the environment on the structure and the calculation of the probability that a pre-defined limit state, which corresponds to an undesired event (e.g. initiation of corrosion, cracking or spalling of concrete cover), will occur. Currently the use of the *fib* Model Code, as well as other probabilistic performance-based design approaches, is still limited in the design of RC structures, whilst deterministic models often implemented in commercial software are more used [9,10]. A more widespread use of probabilistic performance-based models would be extremely useful in order to compare different design solutions, to quantitatively assess the benefits connected with the use of preventative techniques and to determine the reliability of different design combinations. The main limitation to the use of service life models is the lack of knowledge about the realistic nature of their output. Indeed the evaluation of the reliability of service life predictions of reinforced concrete structures is quite a difficult task, since nowadays available models are quite 'young' compared to the length of usual service lives of RC structures and feedback data are not available yet. Attempts have been made to apply the models to existing structures [11-13], but in this case, if the long-term performance can be evaluated through inspection, there is lack of compliance tests used as model inputs. Nevertheless, the lack of experience on the reliability of service life predictions should not be a reason for rejecting any type of modelling. Such an approach, in fact, would leave designers of reinforced concrete structure without any tools for a sound comparison of different design scenarios. This, especially when preventative measures are considered, would lead to irrational choices that may over- or underestimate the role of each solution considered. A wiser approach would be a cautionary use of presently available models, considering them as a summary of the previous experience. Nevertheless, even the use of available models is often more complicated when additional preventative measures, such as corrosion resistant bars, are considered since there is lack of specific parameters.

This paper applies the performance-based approach proposed by the *fib* Model Code for the design of durable RC structures and discusses some critical aspects related to its use. To point out these aspects and provide a guide in the identification of possible options for the durability design, including the use of corrosion resistant reinforcement, the design of a RC element exposed to a marine environment was considered.

2. Design of a RC element in a marine environment

The design of a RC element exposed in the marine splash zone (XS3 exposure class according to EN 206) on the coast of the Mediterranean Sea was simulated. Different design options in terms of types of concrete and reinforcement were considered. As far as the type of concrete is concerned, a Portland cement, OPC (CEM I according to EN 197-1) and a ground granulated blast furnace slag cement, BF (CEM III/B) were taken into account with a water/binder (*w*/*b*) ratio of 0.45, as suggested by the EN 206 standard, which provides guidance on the selection of designated concrete as a function of the exposure environment. Different types of reinforcement were considered: conventional black steel, galvanized steel and stainless steel of grades 1.4307 and 1.4462, i.e. respectively a low carbon austenitic stainless steel with composition of 18% Cr, 8-10% Ni and a duplex stainless steel with composition 22% Cr, 5% Ni, 3% Mo, according to the standard EN 10027. The service life was modelled through the *fib* Model Code and the limit state equation was solved by means of the Monte Carlo simulation method (10^6 simulations were performed for each case).

2.1 Limit state equations

The service life can be defined as the sum of the initiation time, which ends when the steel is depassivated, and the propagation time, which finishes when a given limit state takes place, beyond which consequences of corrosion cannot be further tolerated and a repair work is needed [2]. This distinction between initiation and penetration periods is useful in the design of RC elements, since different processes and variables should be considered in modelling the two phases [6]. For a structure exposed to a chloride-bearing environment, the initiation of corrosion can be assumed as the limit state, since the propagation time is relatively short and it can be neglected [1]. The initiation period is defined as the time required for chlorides to reach a critical threshold at the depth of the outermost steel bars. The probability of failure, p_f, is evaluated as the probability that the initiation limit state function, g, reaches negative values:

$$p_f = P\{g < 0\} = P\{Cl_{th} - Cl(d_c, t_{SL}) < 0\} \qquad (1)$$

where:

Cl_{th} is the critical chloride threshold; d_c is the depth of the outermost rebar; t_{SL} is the target service life; $Cl(d_c,t_{SL})$ is the content of chloride in the concrete at a depth, d_c, and at a time, t_{SL}.

The target service life, t_{SL}, which needs to be defined in the design phase, is guaranteed if the probability of failure p_f is equal or lower than a preset target probability, P_0, which should be also defined in the design phase.

In the *fib* Model Code, the initiation limit state function, g, is evaluated as:

$$g = Cl_{th} - \left\{ C_0 + \left(C_{s,\Delta x} - C_0 \right) \cdot \left[1 - erf \frac{d_c - \Delta x}{2 \cdot \sqrt{D_{app,0} \cdot t}} \right] \right\} \qquad (2)$$

where: C_0 is the initial chloride content of the concrete; Δx is the depth of the convection zone where, beside diffusion process, other mechanisms of chloride penetration can occur; $C_{s,\Delta x}$ is the substitute chloride surface content, C_s, at the depth Δx; $D_{app,0}$ is the apparent coefficient of chloride diffusion through concrete.

The apparent coefficient of chloride diffusion of concrete is determined as:

$$D_{app,0} = k_e \cdot D_{RCM} \cdot k_t \cdot A(t) \qquad (3)$$

where: k_e is the environmental transfer variable and is a function of the temperature of the element (T_{real}); D_{RCM} is the chloride migration coefficient, k_t is a transfer parameter and A(t) is the subfunction considering the 'ageing'.

The subfunction $A(t)$ is evaluated as:

$$A(t) = \left(\frac{t_0}{t} \right)^a \qquad (4)$$

where: t is the time, t_0 is the reference point of time and a the ageing factor.

Since all the functions and parameters involved in this model cannot be reported in this paper, reference to the *fib* Model Code is made for a detailed description [7].

2.2 Selection of values for the design parameters

The parameters involved in equations (2), (3) and (4), the preset target probability, P_0, and the target service life, t_{SL}, need to be determined in the design phase. Some of them should be chosen by the designer (i.e. D_{RCM}, $C_{s,\Delta x}$, Cl_{th}, C_0, T_{real}), whilst others are provided by the model. Table 1 summarises the values of the input parameters, their description, as well as the type of probability density function distribution used for the calculations.

Migration coefficient of chloride, D_{RCM}. For the designed concrete mix the *fib* Model Code suggests to measure D_{RCM} through an experimental test, i.e. the rapid chloride migration test [14]. For the selected types of concrete, experimental data on D_{RCM} published in another work [15], evaluated through the rapid chloride migration test on specimens cured 28 days, were considered (Figure 1). For each type of concrete, a linear relationship between D_{RCM} and water/binder ratio can be observed and from this relationship, for the water/binder ratio equal to 0.45, D_{RCM} equal to $6.5 \cdot 10^{-12}$ and $1.5 \cdot 10^{-12}$ m^2/s respectively for OPC and BF cements were evaluated (Table 1).

Substitute chloride surface content, $C_{s,\Delta x}$. To determine $C_{s,\Delta x}$, the model merely provides a flow chart, with the procedure to be followed, starting from environmental data and material properties and, as an example, a quite complex equation with a limited validity in terms of exposure conditions. These indications are hardly understandable and no quantitative value, to be used in the design phase, is supplied for the various exposure zones. In this work, to determine this parameter, values of surface chloride content, C_s, were collected from data published in the literature, obtained from specimens or structures exposed to splash and tidal zones [16-29] and reported in Table 2. Figure 2 shows the influence on C_s of the exposure time, the type of cement and the climate (only a distinction between temperate and tropical climate was made). In works where different types of concrete were analysed, a dependence of C_s from the type of cement can be observed. For instance, according to Mohammed et al. [20], after 15 years of exposure, a C_s of 3.53% by mass of binder was determined on Portland cement concrete specimens, whilst of 4.12% and 5.8% by mass of binder respectively on ground granulated blast furnace slag and fly ash concrete. Also other authors reported lower values of C_s for Portland cement concrete compared to blended cement concrete, made with fly ash, ground granulated blast furnace slag or silica fume cements, probably due to the higher level of chloride binding [22,25,28]. The influence of water/binder ratio seems to be rather uncertain. For instance, in FA concrete, C_s decreases by decreasing the water/binder ratio, whilst in OPC concrete a clear trend cannot be defined [25]. The limited number of available data, however, does not allow to determine reliable values of C_s for different concrete compositions.

Comparing results of different authors, some dependence of C_s on the exposure time can be observed: for instance, considering only OPC concrete exposed to tropical climates (black circle symbols in Figure 2) an increase of C_s occurred increasing the exposure time. The lowest values, around 2% by mass of binder, were measured after 0.25 years [22], whilst the highest values, higher than 10% by mass of cement, were obtained after more than 40 years of exposure [21]. Therefore, also the dependence on the exposure time cannot be properly addressed.

As far as the effect of the climate, i.e. of temperature and humidity, is concerned, the C_s concentration measured at a given time of exposure in temperate climate (grey symbols in Figure 2) appears to be lower than the concentration measured at the same time in tropical environments (black symbols in Figure 2). For instance, after 5 years of exposure, Luping et al. [19] determined a C_s between 1.26% and 5.7% by mass of binder on specimens exposed to the Swedish coast, whilst Chalee et al. [25] obtained, on specimens exposed in the Thailand Gulf, a concentration between 5.9% and 6.7% by mass of cement. However different types of concrete were considered in the two works and the observed differences might be due to the effect of concrete composition rather than a real effect of climate.

Considering difficulties in defining the role of different factors, in this study the surface chloride content was treated as a time-invariant parameter and the effects of the concrete composition were neglected. By considering the literature data as a whole (to be conservative, where an interval of variation of C_s was present, the maximum values were considered), the cumulative frequency distribution shown in Figure 3 was obtained. This was fitted by a normal distribution (black curve) with an average value of 5% and a standard deviation of 2% of chloride by mass of binder (Table 1). This distribution was then considered representative of $C_{s,\Delta x}$.

Critical chloride threshold, Cl_{th}. For this parameter, the model proposes values only for black steel, without taking into account corrosion resistant steels. Indeed, the choice of suitable values of Cl_{th} for corrosion resistant steel reinforcement is completely demanded to the expert or to literature data.

In this work, to detect suitable values of Cl_{th} for stainless steel bars of grades 1.4307 and 1.4462 and galvanized steel, a literature survey, limited to tests on concrete or mortar specimens, was carried out, and results are summarized in Table 3 [30-48]. Table 3 shows that, often, quite different methodologies were used to determine Cl_{th}; thus, the comparison among results obtained in different studies and between different steel grades is rather difficult. Furthermore, some authors reported only a lower limit value for the critical chloride threshold. For stainless steel of grade 1.4307, Cl_{th} values in the range 1-2% by mass of cement were found by Sorensen et al. [30], whilst Bertolini et al. reported that Cl_{th} was even higher than 8% by mass of cement [41,43]. A mean value of 5% by mass of cement, which is between these extreme situations, was considered reasonable and used to calculate the probability density function (PDF). For 1.4462 stainless steel only lower limit values were available; however, on the basis of experience and tests carried out in solution [32], the corrosion resistance of this grade is higher than that of 1.4307 grade, and, hence a mean value of 8% by mass of cement was considered for this study. For galvanized steel the range of variation of Cl_{th} is quite high (between 0.17% and 4.02% by mass of cement) [45-48], but it is common opinion that its corrosion resistance is higher than that of carbon steel, hence an average value of 1.2% by mass of cement was selected.

Other parameters. For the application of the *fib* model, in this study the initial chloride content of the concrete, C_0, was considered zero for the OPC concrete and equal to 0.2% of chloride by mass of cement for BF concrete (the chlorides are present in the slag due to the manufacturing process), whilst the temperature of the structural elements, T_{real}, was assumed equal to the environmental temperature and a value of 20°C was considered as representative of the average yearly temperature in the Mediterranean area.

As far as the target probability, P_0, is concerned, at the moment there is no general agreement on its meaning [11,12,49], however the model suggests the values for the different limit states and for the serviceability limit state of depassivation, i.e. the initiation of corrosion, a value of 10% is recommended.

Initially a target service life of 100 years was considered and the mean value of concrete cover thickness, d_c, was varied, by steps of 5 mm, from 25 to 150 mm. Then the concrete cover was fixed to 45 mm, that is the value suggested in the Eurocode 2 for this exposure condition, and the target service life was varied between 10 and 150 years.

3. Results and discussion

3.1 Performance-based durability design

Figure 4 shows the probability of failure, p_f, as a function of the mean value of the concrete cover thickness for the two types of concrete and the four different types of reinforcement considered in this work. To detect suitable design options, a maximum value of 10% for the target probability, P_0, was defined (dashed line in Figure 4). Combinations of minimum concrete cover thickness, type of concrete and type of reinforcement which guarantee this target probability for a service life of 100 years can be determined, by the intersection between the target probability, P_0, and the curve of each option. As expected, black steel rebars even in concrete made with ground granulated blast furnace slag cement (BF) and a water/binder ratio of 0.45, required high concrete cover thicknesses (around 90 mm). Such values are hardly feasible in the construction practice. As expected, an even higher concrete cover thickness would be required with OPC concrete, which is characterized by a lower resistance to chloride penetration. Although in this example a harsh exposure condition, i.e. the splash zone, was considered and with black steel bars high values of concrete cover thickness were expected for both types of concrete, it seems that the output values, especially for the Portland cement concrete, are conservative. It is a common opinion that for a Portland cement concrete a concrete cover thickness of 55 mm, as suggested in the European standards, i.e. the EN 206 and the EuroCode 2, is not enough to guarantee a service life of 100 years in this environment and that a higher concrete cover should be adopted. However, according to the model output even values three times higher should be considered.

Figure 4 shows that corrosion resistant steel bars could be taken into account to decrease the concrete cover thickness, besides a decrease of the *w/b* ratio (which has not been considered in this work). With the BF concrete, the minimum value of the concrete cover decreased from 90 mm for black steel bars to 70 mm for galvanized steel and to 25 mm for stainless steel 1.4307. An even lower concrete cover thickness could be used with stainless steel 1.4462. Although several design options may be selected to reach the target probability, the modelling showed that the use of stainless steel bars may be an interesting solution since it allows a significant reduction of the concrete cover thickness to values easily obtainable in practice, avoiding the risk of early cracking due to thermal or drying shrinkage.

The advantages of stainless steel in comparison to other solutions can be better observed in Figure 5, where the probability of failure is shown as a function of the initiation time, assuming a concrete cover thickness of 45 mm. Results show that stainless steel bars may guarantee the target probability of failure with a service life even longer than 150 years, when a BF concrete is used. With stainless steel 1.4462, a long service life could be also reached with OPC concrete. Conversely, with black and galvanized steel, the target probability of failure can be achieved only with service lives respectively less than 10 and 15 years if BF concrete is used. Furthermore, Figure 5 shows that the reliability level strongly varies as a function of the different grades of stainless steel. For instance, for a service life of 100 years, although p_f was lower than the target probability, P_0, for both stainless steel bars, it increased from about 0.35% to 2.65% passing from 1.4462 to 1.4307 stainless steels, making the former solution, to which higher costs are associated, more 'robust' and reliable in relation to durability than the latter.

The results described in this section show that the probabilistic service-life modelling allows to differentiate the various design options and provide a clear ranking, for the environmental actions considered in this example, between the expected performances of galvanized steel and different grades of stainless steel. Even though there is no possibility for the time being to assess the 'realistic' nature of the actual values of the calculated probability of failure, results of the type shown in Figure 4 can help the designers in the selection of an appropriate durability strategy. The role of the input parameters on the output of the model, nevertheless should be better investigated.

3.2 Role of input parameters

The results of the modelling depend on the values of the input parameters both those chosen by the designer and those provided by the model. As described in section 2.2, the selection of appropriate probability distributions of Cl_{th} and $C_{s,\Delta x}$ is the most critical step for the designer, since the model lacks of information. Hence there is a need to assess the effect of these parameters in the output of modelling.

Besides the role of parameters selected by the designers, the reliability of the modelling also depends on the parameters provided by the model. Amongst these, the ageing factor, *a*, which accounts the time dependency of the diffusion coefficient, has been described as one of the most influencing parameter [50-52]. The study of this parameter in the modelling output is crucial when different types of concrete are considered as possible design options. Hence the time dependency of the diffusion coefficient will also be described.

Effect of critical chloride threshold and chloride surface concentration. Since the distribution of the service life can be evaluated through the following equation, determined from equations 2-4:

$$t_i = \left[\frac{x - \Delta x}{2 \cdot \sqrt{k_e \cdot D_{RCM} \cdot k_t \cdot t_0^a}} \cdot \frac{1}{\mathrm{erf}^{-1}\left(1 - \frac{Cl_{th} - C_0}{C_{s,\Delta x} - C_0}\right)} \right]^{\frac{2}{1-a}} \quad (5)$$

it clearly appears that the two parameters Cl_{th} and $C_{s,\Delta x}$ are strictly correlated. Neglecting the influence of C_0, an increase of Cl_{th}, which is a resistance variable, has a comparable effect of a decrease of $C_{s,\Delta x}$, which is a load variable. Hence, to study simultaneously their influence on the service life PDF, the $Cl_{th}/C_{s,\Delta x}$ ratio can be taken into account. At this regard, the knowledge of the probability density function of this ratio is needed. Figure 6 shows the frequency analyses of the $Cl_{th}/C_{s,\Delta x}$ ratio, evaluated considering the values reported in Table 1, for the three types of bars: black, galvanized and 1.4307 stainless steel (only one type of stainless steel was considered). The study of the ratio was achieved through a Monte Carlo system (with approximately 60 000 calculations). For these three examples, the PDF of this ratio was well described through a lognormal distribution with a mean value equal to the ratio between the mean values of Cl_{th} and

$C_{s,\Delta x}$ and a coefficient of variation (CV) equal to 0.5. Although the type of distribution as well as its parameters should be verified for other values of Cl_{th} and $C_{s,\Delta x}$, they were assumed for studying the influence of the $Cl_{th}/C_{s,\Delta x}$ ratio on the output of the model. Figure 7 shows the initiation time as a function of the ratio between Cl_{th} and $C_{s,\Delta x}$, considering a target probability P_0 of 10%, a concrete cover of 45 mm and both OPC and BF concretes. These two examples show that, up to values of the $Cl_{th}/C_{s,\Delta x}$ ratio around 0.8, the correlation between the initiation time and the $Cl_{th}/C_{s,\Delta x}$ ratio is well described by exponential relationships with similar slopes. For values of the $Cl_{th}/C_{s,\Delta x}$ ratio higher than 0.8 a significant increase of the initiation time occurs. The observed exponential trend between t_i and $Cl_{th}/C_{s,\Delta x}$ ratio depends on the trend of the inverse error function, at denominator in the equation (5). As a consequence of this trend, for low values of $Cl_{th}/C_{s,\Delta x}$ ratio a slight variation of the ratio leads to a slight variation of the initiation time; conversely for high values of the $Cl_{th}/C_{s,\Delta x}$ ratio even a slight variation leads to significant variation of the initiation time. The variations of the initiation time, Δt_i (%), can be quantified as:

$$\Delta t_i(\%) = \frac{t_i^* - t_i}{t_i} \cdot 100 \quad (6)$$

where:

t_i is the initiation time evaluated for each $Cl_{th}/C_{s,\Delta x}$ ratio, considering a target probability P_0 of 10% and a concrete cover of 45 mm;

t_i^* is the initiation time evaluated varying by ±10, ±15 and ±20% the $Cl_{th}/C_{s,\Delta x}$ ratio. This $\Delta(Cl_{th}/C_{s,\Delta x})$ ratio accounts for errors in the estimation of one of the two parameters.

Figure 8 shows the variation of initiation time, Δt_i, as a function of the variation of $Cl_{th}/C_{s,\Delta x}$ ratio. It can be observed that the type of concrete has a negligible influence on the variation of initiation time (it should be assessed if this is valid for other concrete compositions as well as other concrete cover thicknesses and target probability P_0). Furthermore Δt_i increases increasing the $Cl_{th}/C_{s,\Delta x}$ ratio: for instance, for BF concrete, a variation of the $Cl_{th}/C_{s,\Delta x}$ ratio of 15% (grey symbols in Figure 8), leads to a Δt_i of about 10% when the $Cl_{th}/C_{s,\Delta x}$ ratio is equal to 0.12 and of about 50% when the $Cl_{th}/C_{s,\Delta x}$ ratio is equal to 0.6. This means that an error in the estimation of the values of the input parameters Cl_{th} and $C_{s,\Delta x}$ has different effects on the evaluated service life as a function of the type of reinforcement. For black steel, characterized by a low value of Cl_{th}, even in fairly unaggressive environments, where the $C_{s,\Delta x}$ is relatively low, the $Cl_{th}/C_{s,\Delta x}$ ratio is quite low and, hence, an inaccuracy in the estimation of both Cl_{th} and $C_{s,\Delta x}$ would have a negligible effect on the service life, as already observed by Ferreira [50]. For galvanized steel in harsh environment the $Cl_{th}/C_{s,\Delta x}$ ratio can be considered still quite low, around 0.24, and an erroneous estimation of these input parameters would have negligible effects; conversely in less aggressive environments the variation in the service life could become significant, even of the order of 30%, since the $Cl_{th}/C_{s,\Delta x}$ ratio could be even higher than 0.4. With stainless steel the situation is even the worst and an inaccurate definition of the input parameters could lead to a strong overestimation or underestimation of the service life: a 10% variation of $Cl_{th}/C_{s,\Delta x}$ ratio could lead to a Δt_i of the order of 40%. Indeed, for stainless steel, the model is quite sensitive to the estimated values of Cl_{th} and $C_{s,\Delta x}$, and it is still inadequate to design RC structures with this type of reinforcement, due to the lack of indications on the critical chloride threshold and for the chloride surface concentration values and to the difficulty in defining reliable values for them. As a matter of fact, Tables 2 and 3 show that the chloride surface concentration and chloride threshold values reported in the literature are extremely variable and they do not allow a reasonable estimation of the PDF of these parameters.

Since the difficulties in defining reliable values for the input parameters clearly limit a widespread use of the model, there is the need to update it in order that it becomes a really useful and user-friendly tool for the design of durable structures. For instance, a procedure to estimate the critical chloride threshold for stainless steels should be found. Following the approach proposed by the *fib* Model Code to assess the apparent coefficient of chloride diffusion of concrete, even the chloride threshold under real exposure conditions, $Cl_{\mathrm{th,field}}$, could be determined through a compliance test, $Cl_{\mathrm{th,test}}$. The result of such a test should be modified through the use of appropriate corrective parameters to predict the behaviour of steel in a real environment and to take into account the role of the factors (i.e. temperature, pH of pore solution ...) which can affect it. Unfortunately this is a quite complicated task (a standardized methodology to evaluate the critical chloride threshold is not available yet, even for carbon steel). In fact, the high chloride threshold of corrosion resistant bars, in practice, does not allow the use of conventional tests based on the penetration of chloride through concrete specimens, since testing times would be extremely long even for small concrete cover thickness. Studies are being carried out, by means of laboratory tests, to investigate on possible procedures for the evaluation of Cl_{th} based on mixed-in chloride and potentiostatic polarization, and to define the corrective parameters [53].

As far as the surface chloride concentration is concerned, even this parameter should be evaluated by means of an experimental test. For instance, the Life-365 model suggests to determine it through the method proposed in the ASTM C1556 standard, which consists in exposing a concrete specimen in an aqueous NaCl solution, prepared with a NaCl concentration of 165 g/L, for a certain period of time, i.e. at least 35 days [54]. However, the result of this tests, as well as of other tests proposed in the literature to evaluate the chloride resistance of concrete, e.g. the EN 12390-11 standard, could not be considered representative of real exposure conditions and directly used in a predictive model, but should be modified with corrective parameters. Unfortunately, at the moment, no studies provide information at this regard. A first step in this direction should be the collection of data both from existing structures and laboratory data as well as the definition of the dependence on the factors which affect the surface chloride concentration, i.e. the concrete composition and the environmental exposure, and the evaluation of empirical correlations with other concrete proprieties, i.e. the resistance to chloride diffusion.

Time dependency of the diffusion coefficient. It is well know that a reduction of the diffusion coefficient in time is due to the progress of cement hydration with the consequent expansion of the volume of hydration products and reduction of capillary porosity, and that the degree of reduction of the diffusion coefficient depends on the type of binder, being each binder characterized by a different kinetic of hydration. The ageing factor, which takes account of the reduction of the diffusion coefficient, has a strong impact on the prediction of the service life. Figure 9 shows the cumulative distribution function of the A(t) subfunction considering the "ageing" (equation 4), taking into account t equal to 100 years and a values of 0.3 and 0.45 as proposed by the *fib* model for OPC and BF concrete respectively (besides these two concretes, the model proposes an a value of 0.6 for FA concrete, whilst it does not consider other types of concrete). Considering the 50th percentile, i.e. the median value, A(t) decreases from 0.1 for OPC concrete to 0.035 for BF concrete, leading to a decrease of the initial D_{RCM} of one order of magnitude after 100 years for OPC concrete and more than one and a half order of magnitude for blended cement concrete. Hence, it can be inferred that the significant differences in the service life prediction between OPC and BF concrete accounted in this work (Figure 5) are mainly due to the different ageing factor rather than the different resistance to chloride penetration, i.e. to the diffusion coefficient. Therefore an accurate determination of the a factor is a crucial aspect for the correct prediction of service life.

In general, most of the authors agree that the reduction of the diffusion coefficient of blended cements, e.g. ground granulated blast furnace slag or fly ash, is higher than for Portland cement [55-58]. However, Audenaert et al. [59] reported that for ordinary concrete the ageing factor is independent of the cement type. Nevertheless highly different values of ageing factors have been proposed in the literature for the same type of cement. For instance, for OPC concrete, Thomas et al. [56] determined, through long-term field and laboratory studies, an ageing factor of 0.14, Stanish et al. [57] obtained, by means of 4-year laboratory tests, a value of 0.32, Nokken at al. [58] got values of the order of 0.57, through three years bulk diffusion ponding tests, Mangat et al. [55] found ageing factors between 0.44 and 0.74, depending on the water/cement ratio; conversely according to [52] OPC concrete did not exhibit a decrease of the diffusion coefficient with time, even after 2 years of ponding tests. For FA concrete, several authors reported ageing factors values around 0.7 [56-58], whilst other authors [52,55] determined values around 1. For BF concrete, high values of the ageing factors, i.e. higher than 1, were determined, [55,56] conversely values of the order of 0.2 were found by Audenaert et al. [59]. These observed differences in the ageing factors could be, however, due to the different experimental methodologies used to determine it, to the duration of the experimental exposure time or to the values used as the time basis (t_0 in equation 4). Due to this strong variability in values proposed in the literature as well as to the great impact on the service life prediction, as previously discussed, further studies are required to define appropriate ageing factors both for Portland, blast furnace slag and fly ash cements and also for other binder types, which are available in the market and which presently are not considered in the model.

4. Conclusions

In this paper, the performance-based approach proposed by the *fib* in the "Model Code for Service Life Design" has been investigated and applied to the design of a RC element exposed in a marine environment. On the basis of the results the following conclusions can be drawn.

1. Service life modelling allowed to quantify advantages related to the use of different strategies to prolong the service life of RC structures, and to determine the increase in reliability associated to the use of corrosion resistant reinforcement. Nevertheless it also highlighted difficulties in the evaluation of benefits of this preventative technique.

2. Unfortunately, at the moment, the model does not provide sufficient indications for the determination of some input parameters, in particular the surface chloride concentration and the critical chloride threshold for bars different from ordinary black steel and their estimation is demanded to the experience of the designer. A literature survey showed that the definition of proper values for the critical chloride threshold for corrosion resistant steels and for the surface chloride concentration is rather difficult.

3. An error in the estimation of the values of the input parameters Cl_{th} and $C_{s,\Delta x}$ has different effects on the evaluated service life as a function of the type of reinforcement. With black and galvanized steel, an inaccuracy in the estimation of both parameters may have a negligible effect on the outcome of the model. Conversely with stainless steel even small variations may lead to significant changes in the modelled service life.

4. The model prediction is significantly affected by the ageing factor, leading to a decrease of the initial D_{RCM}, after 100 years, of one order of magnitude for Portland cement concrete and more than one and a half order of magnitude for blast furnace slag concrete. Since highly different values of ageing factors have been proposed in the literature even for the same type of cement, further studies are required to set appropriate values for this parameter for a more accurate prediction of service life of concrete structures.

Acknowledgements

The work was supported by the European Union Research Council via a research grant (FP7-PEOPLE-2011-IRSES-294955).

References

[1] Bertolini L, Elsener B, Pedeferri P, Redaelli E, Polder R. Corrosion of steel in concrete – Prevention, diagnosis, repair. 2nd ed. Weinheim: Wiley VCH; 2013.

[2] Tuutti K. Corrosion of steel in concrete. Stockholm: Swedish foundation for concrete research; 1982.

[3] Page CL, Treadaway KWJ. Aspects of the electrochemistry of steel in concrete. Nature 1982;297:109-16.

[4] Arup H. The mechanisms of the protection of steel by concrete. In: Crane AP, editor. Corrosion of reinforcement in concrete construction, Chichester: Hellis Horwood Ltd.; 1983, p. 151-7.

[5] Schiessl P, editor. Corrosion of steel in concrete, Rilem report 60-CSC, London: Chapmann & Hall; 1988.

[6] Bertolini L. Steel corrosion and service life of reinforced concrete structures. Struct Infrastruct E 2008;4:123-37.

[7] International Federation for Structural Concrete, *fib*, 'Model code for service life design', Bulletin n° 34; 2006.

[8] Rahimi A, Gehlen C, Reschke T, Westendarp A. Approaches for Modelling the Residual Service Life of Marine Concrete Structures, International Journal of Corrosion 2014;2014:1-11.

[9] Vořechovská D, Teplý B, Chromá M. Probabilistic assessment of concrete structure durability under reinforcement corrosion attack, J Perform Constr Facil 2010;24:571-9.

[10] Marques PF, Costa A, Lanata F. Service life of RC structures: chloride induced corrosion: prescriptive versus performances-based methodologies, Mater Struct 2012;45: 277-96.

[11] Bertolini L, Lollini F, Redaelli E, Durability design of reinforced concrete structures, Proceedings of Institution of Civil Engineers: Construction Materials 2011;164:273-82.

[12] Bertolini L, Lollini F, Redaelli E, Analysis of the parameters affecting probabilistic predictions of initiation time for carbonation-induced corrosion of reinforced concrete structures, Mater Corros 2012;63:1059-68.

[13] Gehlen C, Sodeikat C. Maintenance Planning of Reinforced Concrete Structures: Redesign in a Probabilistic Environment, Inspection, Update and Derived Decision Making. In Burn S, editor. Proceedings of the 9th International Conference: Durability of Building Materials and Components, Brisbane (Australia), 2002.

[14] NT Build 492, Concrete, mortar and cement-based repair materials: chloride migration coefficient from non-steady state migration experiment, NORDTEST; 1999.

[15] Bertolini L, Lollini F, Redaelli E. Comparison of resistance to chloride penetration of different types of concrete through migration and ponding tests. In: Andrade C, Mancini G, editors. Modelling of corroding concrete structures, Springer; 2011, p. 125-35.

[16] Berke NS, Hicks MC. Predicting chloride profiles in concrete. Corrosion 1994;50:234-9.

[17] Amey SL, Johnson DA, Miltenberger MA, Farzam H. Predicting the service life of concrete marine structures: an environmental methodology. ACI Struct J 1998;95:205-14.

[18] MGee R. Modelling of chloride ingress in Tasmanian bridges. Testing and modelling of chloride ingress in concrete, Bagneux: RILEM Publications S.A.R.L.; 2000, p. 149-59.

[19] Luping T, Andersen A. Chloride ingress data from five years field exposure in a swedish marine environment. In: Andrade C, Kropp J, editors. Testing and modelling of chloride ingress in concrete, Bagneux: RILEM Publications S.A.R.L.; 2000, p. 105-19.

[20] Mohammed TU, Yamaji T, Hamada H. Chloride diffusion, microstructure, and mineralogy of concrete after 15 years of exposure in tidal environment. ACI Mater J 2002;99:256-63.

[21] Tronconis de Rincón O, Castro P, Moreno EI, Torres-Acosta AA, Morón de Bravo O, Arrieta I et al. Chloride profiles in two marine structures – meaning and some predictions. Build Environ 2004;39:1065-70.

[22] Ghods P, Chini M, Alizadeh R, Hoseini M. The effect of different exposure conditions on the chloride diffusion into concrete in the Persian Gulf region. In: Banthia N, Oumoto T, Benturt A, Shah SP, editors. Proceedings of the ConMAT Conference, University of British Columbia, Vancouver (Canada), 2005.

[23] Oh BH, Jang SY. Effects of materials and environmental parameters on chloride penetration profiles in concrete structures. Cement Concrete Res 2007;37:47-53.

[24] Song H-W, Lee C-H, Ann KY, Factors influencing chloride transport in concrete structures exposed to marine environments. Cement Concrete Comp 2008;30:113-21.

[25] Chalee W, Jaturapitakkul C, Chindaprasirt P. Predicting the chloride penetration of fly ash concrete in seawater. Mar Struct 2009;22:341-53.

[26] Oslakovic IS, Bjegovic D, Mikulic D. Evaluation of service life design models on concrete structures exposed to marine environment. Mater Struct 2010;43:1397-412.

[27] Chalee W, Ausapanit P, Jaturapitakkul C. Utilization of fly ash concrete in marine environment for long term design life analysis. Mater Design 2010;31:1242-9.

[28] Pack SW, Jung MS, Song HW, Ann KY, Prediction of time dependent chloride transport in concrete structures exposed to a marine environment. Cement Concrete Res 2012;40:302-12.

[29] Salta M, Melo A, Ricardo J, Póvoa. Chloride profiles in a coastal bridge. Struct Infrastruct E 2012;8:583-94.

[30] Sorensen B, Jensen P B, Maahn E. The Corrosion Properties of Stainless Steel Reinforcement. In: Page CL, Treadaway KWJ, Bamforth PB, editors. Corrosion of Reinforcement in Concrete. Elsevier Applied Science; 1990, p. 601-10.

[31] Pastore T, Pedeferri P. Corrosion Behaviour of a Duplex Stainless Steel in Chloride Contaminated Concrete. Proc. Int. Conf. on Stainless Steel, ISIJ, Chiba; 1991, p. 351-8.

[32] Rasheeduzzafar, Dakhil FH, Bader MA, Khan MM. Performance of Corrosion Resisting Steels in Chloride-Bearing Concrete. ACI Mater J 1992;89:439-48.

[33] Bertolini L, Gastaldi M, Pastore T, Pedeferri MP. Corrosion Behaviour of Stainless Steels in Chloride Contaminated and Carbonated Concrete. Internationale Zeitschrift für Bauinstandsetzen und Baudenkmalpfledge 2000; p. 273-92.

[34] Bertolini L, Gastaldi M, Pedeferri MP, Pedeferri P. Stainless Steel in Concrete. Annual Progress Report, European Community, COST 521 Workshop, Belfast; 2000, p. 27-32.

[35] Bertolini L, Gastaldi M, Pedeferri P, Redaelli E. Factors influencing the corrosion resistance of austenitic and duplex stainless steel bars in chloride bearing concrete. 15th International Corrosion Congress - ICC, Granada, 2002.

[36] Bertolini L, Gastaldi M, Pedeferri P. Stainless Steel in Concrete. Annual Progress Report, European Community, COST 521 Workshop, References 269, Tampere, 2001.

[37] Clemena GG, Virmani YP. Comparing the Chloride Resistances of Reinforcing Bars. Concr Int 2004;26:39-49.

[38] Trejo D, Pillai RG. Accelerated Chloride Threshold Testing—Part II: Corrosion-Resistant Reinforcement. ACI Mater J 2004;101:57-64.

[39] García-Alonso MC , González JA, Miranda J, Escudero ML, Correia MJ, Salta M et al. Corrosion behaviour of innovative stainless steels in mortar. Cement Concrete Res 2007;37:1562-9.

[40] Hartt WH, Powers RG, Kessler RJ. Performance of corrosion resistant reinforcements in concrete and application of results to service life projection, Corrosion 2009, NACE, Houston, 2009, Paper No. 09206.

[41] Bertolini L, Gastaldi M. Corrosion resistance of low-nickel duplex stainless steel rebars. Mater Corros 2011;62:120-9.

[42] Sederholm B, Almqvist J, Randström S. Corrosion Properties of Stainless Steels as Reinforcement in Concrete in Swedish Outdoor Environment, Corrosion 2009, NACE, Houston, 2009, Paper No. 09203.

[43] Gastaldi M, Bertolini L. Effect of temperature on the corrosion behaviour of low-nickel duplex stainless steel bars in concrete. Cement Concrete Res. 2014;56:52-60.

[44] Nurnberger U, Beul W, Onuseit G. Corrosion Behaviour of Welded Stainless Reinforcing Steel in Concrete. Otto Graf Journal 1993;4: 225-59.

[45] Yeomans SR. Performance of Black, Galvanized, and Epoxy-Coated Reinforcing Steels in Chloride-Contaminated Concrete. Corrosion 1994;50:72-81.

[46] Darwin D, Browning JA, O'Reilly M, Xing L, Ji J. Critical Chloride Corrosion Threshold of Galvanized Reinforcing Bars. ACI Mater J 2009;106:176-83.

[47] Maldonado L. Chloride threshold for corrosion of galvanized reinforcement in concrete exposed in the mexican Caribbean. Mater Corros 2009;60:536-9.

[48] Bellezze T, Malavolta M, Quaranta A, Ruffini N, Roventi G. Corrosion behaviour in concrete of three differently galvanized steel bars. Cement Concrete Comp 2006;28:246-55.

[49] Gulikers J. Critical issues in the interpretation of results of probabilistic service life calculations, Proceedings of the International RILEM Workshop on Integral Service Life Modelling of Concrete Structures. Ferreira RM, Gulikers J, Andrade C, editors. Bagneux: RILEM Publications S.A.R.L.; 2007, p. 195-204.

[50] Ferreira RM. Implication on RC structure performance of model parameter sensitivity: Effect of chloride. J Civ Eng Manag 2012;561-6.

[51] Song H-W, Pack S-W, Ann KY, Probabilistic assessment to predict the time to corrosion of steel in reinforced concrete tunnel box exposed to sea water. Constr Build Mater 2009;23:3270-8.

[52] Andrade C, Castellote M, d'Andrea R. Measurement of ageing effect on the chloride diffusion coefficients in cementitious matrices. J Nucl Mater 2011;412:209-16.

[53] Gastaldi M, Lollini F, Bertolini L. Performance-based durability design of reinforced concrete structures with stainless steel bars. La Metallurgia Italiana 2014;7/8:17-21.

[54] Ehlen MA, Kojundic A N, Life-365 v2.2 – Adding user estimates of chloride exposure, Concrete International, 2014.

[55] Mangat PS, Molloy BT. Prediction of long term chloride concentration in concrete. Mater Struct 1994;27:338-46.

[56] Thomas MDA, Bamforth PB. Modelling chloride diffusion in concrete. Effect of fly ash and slag. Cement Concrete Res 1999;29:487-95.

[57] Stanish K, Thomas M. The use of bulk diffusion test to establish time-dependent concrete chloride diffusion coefficients. Cement Concrete Res 2003;33:55-62.

[58] Nokken M, Boddy A, Hooton RD, Thomas MADA. Time dependent diffusion in concrete – three laboratory studies. Cement Concrete Res 2006;36:200-7.

[59] Audenaert K, Yuan Q, De Shutter G. On the time dependancy of the chloride migration coefficient in concrete. Constr Build Mater 2010;24:396-402.

Table 1 Values of the input parameters and types of probability density function distribution, *PDF*, (BetaD = beta distribution; ND = normal distribution; D = deterministic) used for the design of a RC element exposed in a splash marine zone (grey cells indicate parameters chosen by the designer).

Parameter		*Unit*	*Description*	*PDF*	*Option*	*Mean value*	*Standard deviation*
Cl_{th}		% by mass of cement	critical chloride threshold	BetaD $0.2 \leq Cl_{th} \leq 2$	black steel	0.6	0.15
				BetaD $0.6 \leq Cl_{th} \leq 3$	galvanized steel	1.2	0.3
				BetaD $2 \leq Cl_{th} \leq 8$	1.4307 stainless steel	5	1.25
				BetaD $3 \leq Cl_{th} \leq 13$	1.4462 stainless steel	8	2
$C_{s,\Delta x}$		% by mass of cement	chloride content at a depth Δx	ND	-	5.0	2.0
C_0		% by mass of cement	initial chloride content	D	OPC	0	-
					BF	0.2	-
d_c		mm	concrete cover	ND	-	to be determined	10
Δx		mm	depth of the convection zone	BetaD $0 \leq \Delta x \leq 50$	-	8.9	5.6
k_e	b_e	K	regression variable	ND	-	4800	700
	T_{real}	K	temperature of the structural element	ND	-	293	10
	T_{ref}	K	standard test temperature	D	-	293	-
D_{RCM}		10^{-12} m^2/s	chloride migration coefficient	ND	OPC	6.5	1.3
					BF	1.5	0.30
A(t)	a	-	ageing exponent	BetaD $0 \leq a \leq 1$	OPC	0.3	0.12
					BF	0.45	0.2
	t_0	years	reference time	D	-	0.0767	-
t_{SL}		years	target service life	D	-	to be determined	-

Table 2 Reported values of the surface chloride content, C_s, of concrete structures and specimens exposed to marine environments.

C_s[1] (% vs cem)	Time (Years)	*Exposure*	*concrete composition*[2]		*References*
			Binder	*w/b*	
5.1	un.	Structure (splash/tidal)	un.	un.	[16][3]
5.43	un.	Structure (splash) – Atlantic ocean	un.	un.	[17][3]
0.53-7.23	20-62	Structures (tidal) - Tasmania	un.	un.	[18]
3.3	5-5.4	Specimens (splash) - Sweden	OPC	0.4	[19]
1.92-4.68			SRPC	0.3-0.5	
1.26-5.70			95%SRPC+5%SF	0.25-0.5	
2.84			90%SRPC+10%SF	0.3	
3.08			80%SRPC+20%FA	0.3	
1.63			85%SRPC+10%FA	0.35	
3.53	15	Specimens (tidal pool) – near Japan coast	OPC	0.45	[20]
4.12			BF		
5.8			FA		
10.5	38	Structure (splash/tidal) - Maracaibo	OPC	0.44	[21]
11.8	64	Structure (splash/tidal) - Mexico	OPC	0.5-0.6	
1.62	0.25	Specimens (tidal) – Persian Gulf	OPC	0.4	[22]
2.31				0.5	
4.88			OPC+7.5%SF	0.4	
2.78				0.5	
4.86			OPC+12.5%SF	0.4	
4.95				0.5	
3.75		Specimens (splash) – Persian Gulf	OPC	0.4	
4.53				0.5	
5.62			OPC+7.5%SF	0.4	
6.74				0.5	
7.33			OPC+12.5%SF	0.4	
9.43				0.5	
8.54	10	Structure (tidal) - Korea	OPC	0.5	[23]
0.83-5.23	23-58	Structure (splash)	OPC	un.	[24][3]
2.39-6.41		Structures (tidal)			
1.50-3.10	24	Structures (splash/tidal) - Singapore	OPC	0.5	[24][3]
6.2	5	Specimen (tidal) – Thailand Gulf	OPC	0.65	[25]
6.0				0.55	
6.4				0.45	
6.7			FA	0.65	
6.5				0.55	
5.9				0.45	
2.27	25	Structure (splash) – Adriatic coast	BF	0.36	[26]
8	7	Specimen (tidal) – Thailand Gulf	OPC	0.65	[27]
7			FA		
2.05	0.65	Structure (tidal) – South Korea	OPC	0.38	[28]
2.1	2.22			0.39	
2.3	8.99			0.43	
2.1	22.54			0.47	
2.7	44.36			0.42	
2.31	1.35		BF	0.38	
2.5	2.77			0.40	
2.62	8.33			0.44	
2.61	11.36			0.42	
3.09	25	Structure (tidal) – Portugal coast	un.	un.	[29]
2.5		Structure (splash) - Portugal			

[1]when the mix design was unknown, 350 kg/m^3 of binder content and 2300 kg/m^3 of hardened concrete density were considered to express results as % by mass of binder. [2] un. = unknown. [3] values from literature data.

Table 3 Reported values of the critical chloride threshold, Cl_{th}, for different types of reinforcement.

Steel		*Cl_{th}*	*Experimental details*			*Concrete composition*			*Corrosion detection*[5]	*Ref.*
Type	*cond*[1]	*(% bw)*	*Cl^-* [2]	*Exposure conditions*	*Time (year)*	*binder*[3]	*w/b*	*pH*[4]		
1.4307	U	> 8	Mix	outdoor	5	M-SRPC	un.	un.	CVO	[30]
	W	5-8	Mix	outdoor	5	M-SRPC	un.	un.	CVO	[30]
	U	3.5-5	Mix	-	-	M-SRPC	un.	un.	PT	[30]
	W	1-2	Mix	-	-	M-SRPC	un.	un.	PT	[30]
	un.	> 3	Mix	outdoor	1.5	C	un.	un.	EM	[31]
	un.	>4.8	Mix	outdoor	7	C	0.45	un.	CVO	[32]
	un.	> 6	Mix	outdoor + lab: T= 40°C RH = 90-95%	1.6 + 0.8	C-OPC	0.5	A	EM	[33]
	un.	> 4	Mix	outdoor + lab: T= 40°C RH = 90-95%	1.6 + 0.8	C-OPC	0.5	C	EM	[33]
	W	4	Mix	lab: T= 40°C RH = 90-95%		C	un.	A	EM	[34]
	un.	> 5	Mix	lab: 10 < T < 40°C; 60% < RH <95%	0.66	C-CA;BF	0.55	A	EM	[35]
	un.	> 6	D	ponding NaCl	-	C-CA;BF	0.55	A	EM	[36]
	un.	> 5	D	ponding NaCl	-	C-CA;BF	0.55	C	EM	[36]
	un.	> 4.6	D	ponding NaCl	3.6	C	0.5	un.	EM	[37]
	un.	1.23	AT	-	-	M-OPC	0.5	un.	EM	[38]
	un.	> 5	Mix	wet/dry	3	M	0.3	un.	EM	[39]
	un.	> 6	D	ponding NaCl	-	C	0.41-0.5	un.	EM	[40]
	un.	> 8	Mix	lab: T =20°C RH=90%	-	C-CA	0.5-0.65	A	EM	[41]
	un.	> 3	Mix	outdoor	2	un.	0.5	C	EM	[42]
	un.	> 8	Mix	lab: T =40°C RH=90%	-	C-CA	0.5-0.65	A	EM	[43]
1.4462	un.	>2.5	Mix		-	C		C	EM	[44]
	un.	>4.5	Mix		-	C		A	EM	[44]
	un.	> 5	Mix	lab: 10 < T < 40°C; 60% < RH <95%		C-CA;BF	0.55	A	EM	[35]
	un.	> 6	D	ponding NaCl	-	C-CA;BF	0.55	A	EM	[36]
	un.	> 3	Mix	outdoor	2	un.	0.5	C	EM	[42]
galv.	un.	>0.17	D	wet/dry	0.36	C-OPC	0.8	un.	EM	[45]
	un.	>0.15	D	salt fog	0.36	C-OPC	0.8	un.	EM	[45]
	un.	< 0.6	Mix	outdoor	7	C	0.45	un.	CVO	[32]
	un.	0.43	D	wet/dry		C	0.45	un.	EM	[46]
	un.	0.3-0.7	D	outdoor	9	C-OPC	0.4-0.7	un.	EM	[47]
	un.	1.36-4.02	D	wet/dry	0.5	C-OPC (low alkali)	0.55	un.	EM	[48]

un. = unknown. [1] surface steel condition: W/U = welding/unwelding. [2] Method of chloride introduction: Mix = mixed in; D = diffusion; AT = accelerated chloride transport. [3] C/M =concrete/mortar; SRPC = sulphate resisting portland cement; CA = limestone cement; BF = ground granulated blast furnace slag; OPC = portland cement. [4] A/C = alkaline/carbonated. [5] EM = electrochemical measurements; CVO = cracks visual observation; PT = potentiostatic test.

Figures

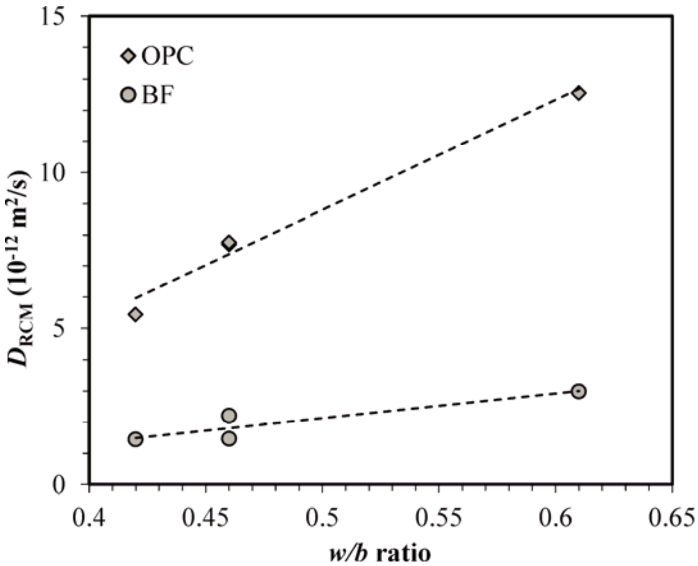

Figure 1 Chloride diffusion coefficient, D_{RCM}, measured through the rapid chloride migration test on specimens cured 28 days, as a function of water/binder (*w*/*b*) ratio and type of binder (OPC = Portland cement; BF = ground granulated blast furnace slag cement) [15].

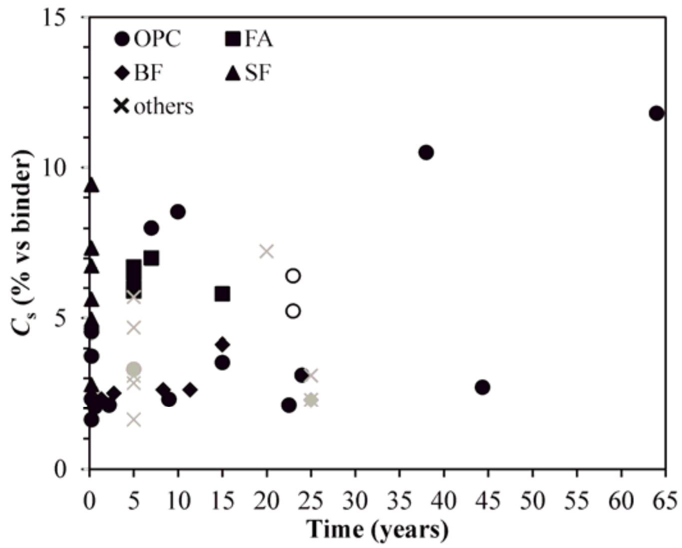

Figure 2 Chloride surface concentration, C_s, as a function of the exposure time, the type of binder (OPC = Portland cement; FA = fly ash; BF = ground granulated blast furnace slag; SF = silica fume; others = other types of binder, e.g. ternary binder) and the climate (black symbols: tropical; grey symbols: temperate; white symbols: unknown) [16-29].

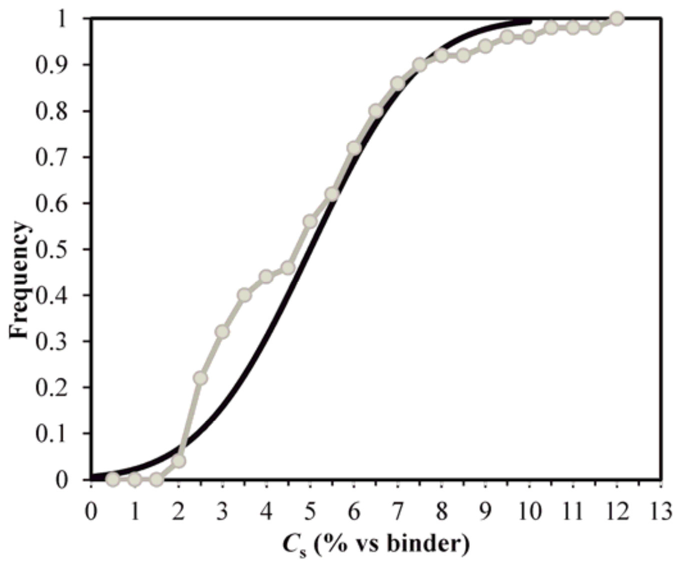

Figure 3 Cumulative frequency distribution of literature data of chloride surface concentration, C_s, reported in Table 2 (grey symbols) and cumulative density function assumed in the calculation (black line).

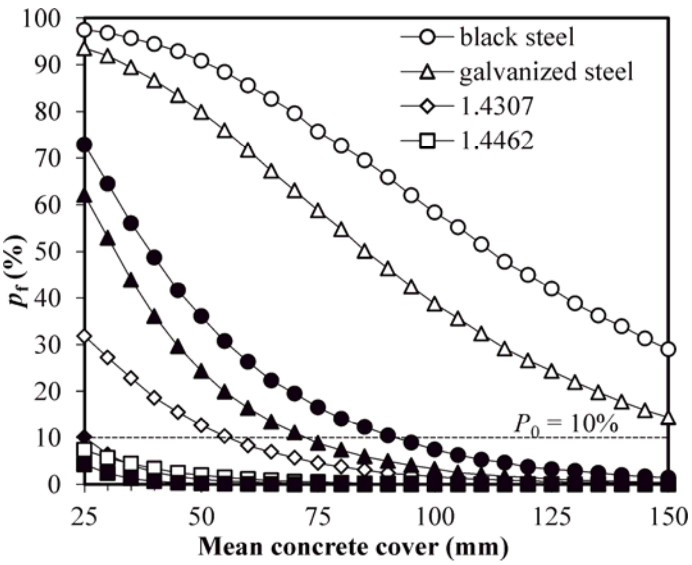

Figure 4 Probability of failure, p_f, as a function of mean concrete cover thickness, the type of reinforcement and the type of binder (OPC = white symbols; BF = black symbols) for a target service life of 100 years.

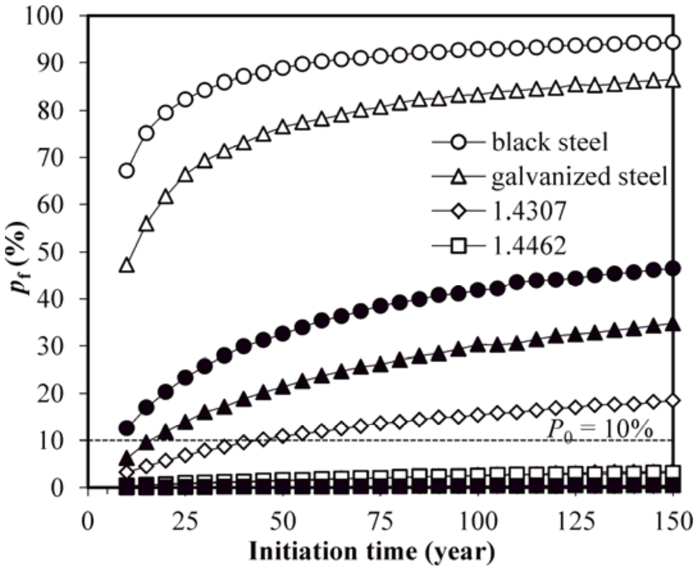

Figure 5 Probability of failure, p_f, as a function of the initiation time, the type of reinforcement and the type of binder (OPC = white symbols; BF = black symbols) considering a concrete cover thickness of 45 mm.

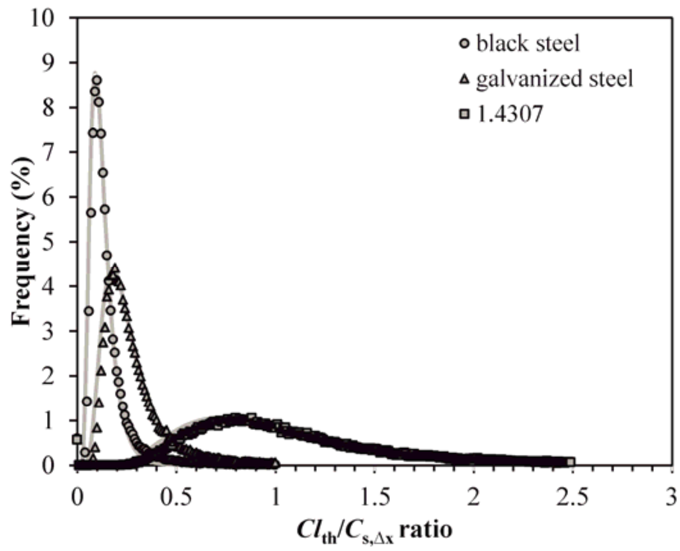

Figure 6 Frequency analysis of the $Cl_{th}/C_{s,\Delta x}$ ratio for black, galvanized and stainless steel of grade 1.4307 and interpolation with lognormal probability density functions (values of Cl_{th} and $C_{s,\Delta x}$ reported in Table 1 were considered to study the $Cl_{th}/C_{s,\Delta x}$ ratio).

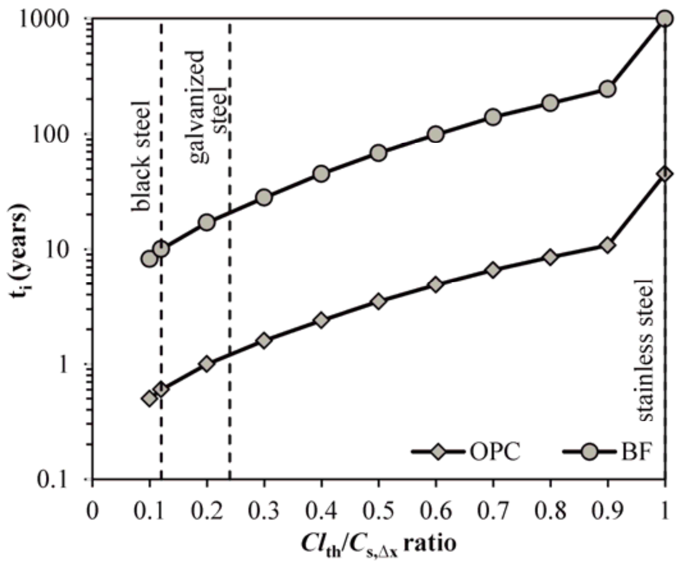

Figure 7 Initiation time as a function of the $Cl_{th}/C_{s,\Delta x}$ ratio for OPC and BF concrete, assuming a concrete cover thickness of 45 mm and a target probability P_0 of 10%. The dashed lines indicate the mean values of the $Cl_{th}/C_{s,\Delta x}$ ratio for black, galvanized and stainless steels.

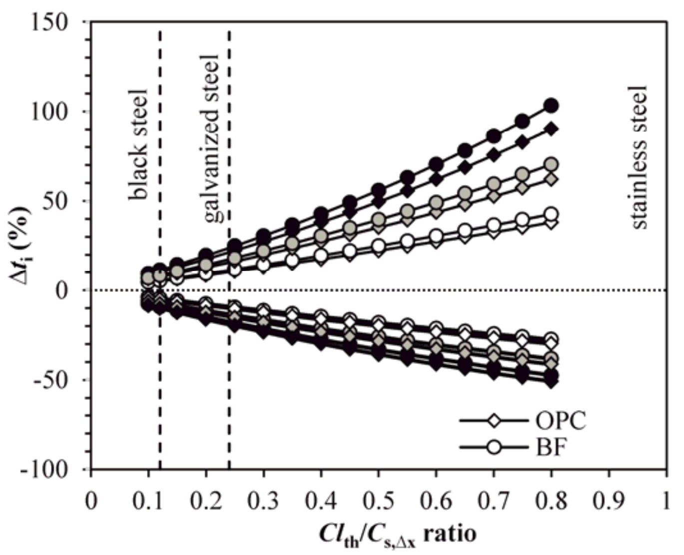

Figure 8 Variation of the initiation time, Δt_i, as a function of the variation of $Cl_{th}/C_{s,\Delta x}$ ratio (white symbols: ±10% variation; grey symbols: ±15% variation; black symbols: ±20% variation) for OPC and BF concrete, assuming a concrete cover thickness of 45 mm and a target probability P_0 of 10%. The dashed lines indicate the mean values of the $Cl_{th}/C_{s,\Delta x}$ ratio for black, galvanized and stainless steels.

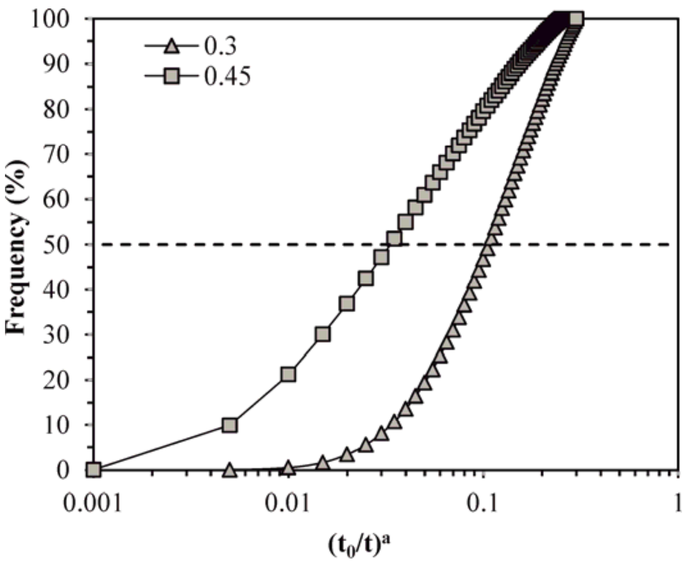

Figure 9 Frequency analysis of the subfunction $A(t) = (t_0/t)^a$, considering, for the ageing factor *a*, the values of 0.3 (suggested by the *fib* model for portland cement) and 0.45 (suggested by the *fib* model for ground granulated blast furnace slag cement) and *t* equal to 100 years.